

# Method for determining the lifetimes of the long-lived $1s2s2p\ ^4P_J$ state J-levels

Cite as: AIP Conference Proceedings **2075**, 200001 (2019); <https://doi.org/10.1063/1.5091426>  
Published Online: 26 February 2019

S. Nanos, and E. P. Benis



[View Online](#)



[Export Citation](#)

**AIP | Conference Proceedings**

**Get 30% off all print proceedings!**

Enter Promotion Code **PDF30** at checkout



AIP Publishing

# Method for Determining the Lifetimes of the Long-lived $1s2s2p\ ^4P_J$ State $J$ -levels

S. Nanos<sup>1,a)</sup> and E.P. Benis<sup>1</sup>

<sup>1</sup>*Department of Physics, University of Ioannina, GR 45110 Ioannina, Greece.*

a)<sup>a</sup>Corresponding author: snanos@cc.uoi.gr

**Abstract.** A method is proposed for measuring the  $J$ -level lifetimes of the long-lived  $1s2s2p\ ^4P_J$  state for low  $Z$  Li-like ions. This necessity stems from the fact that in Auger electron spectroscopy it is necessary to accurately determine the effective detection solid angle that straightforwardly depends on the lifetimes of the long-lived states. The proposed method is applied to the geometry of the zero-degree projectile electron spectroscopy (ZAPS) setup, located at the NCSR "Demokritos" Tandem accelerator laboratory, utilizing Monte Carlo type simulations within the SIMION ion optics package. It is found that the proposed method can be safely applied to elements having  $5 \leq Z \leq 9$ .

## INTRODUCTION

Over the last few decades, considerable progress has been made in obtaining information on both the atomic structure and collision dynamics of multiply excited atomic states using high resolution Auger electron spectroscopy [1]. The determination of highly accurate excitation energies, transition rates, and lifetimes combined with production cross section information obtained from line intensity measurements leads to a better overall understanding of the dominant processes at play. Recently, interest has been focused in the long-lived  $1s2s2p\ ^4P_J$  state, usually termed *metastable*, investigated by high energy resolution techniques such as the zero-degree projectile electron spectroscopy (ZAPS) [2, 3, 4, 5, 6]. A persistent problem in such measurements is the determination of the contribution from metastable states to the measured Auger electron yields due to their inherent long lifetimes [7, 8, 9]. Indeed, in ZAPS setups, where the electron spectrometer lies in the path of the projectile and the electrons are measured at zero degrees with respect to the beam direction, the excited long-lived ionic states, such as the  $1s2s2p\ ^4P_J$  examined here, decay throughout the path of the ionic beam towards the spectrometer, and even through it. Therefore the overall electron detection solid angle varies significantly with the position of electron emission, resulting in an important correction to the measured electron yields. Such corrections have been reported in the literature for various experimental stations [10, 3], as well as for the ZAPS setup utilized here [11, 12], using theoretically calculated lifetimes for the  $J$ -levels of the  $1s2s2p\ ^4P_J$  state. As shown in Table 1, the reported values for the  $J$ -levels lifetime may differ significantly in certain cases (e.g.  $J = 3/2$ ). Thus, this work focuses on the description of a new method for *experimentally* determining the lifetimes of the  $J$ -levels of the  $1s2s2p\ ^4P_J$  long-lived state. The method is implemented in the SIMION ion optics simulation environment for the geometry of the high resolution electron spectroscopy ZAPS setup, currently located at the NCSR "Demokritos" Tandem accelerator laboratory.

## PRINCIPLE OF THE METHOD

The proposed method is examined using the  $1s2s2p\ ^4P_J$  states of  $C^{3+}$  due to the recent interest on the formation of the Li-like states in collisions of mixed ( $1s^2$ ,  $1s2s\ ^3S$ ) state He-like carbon with gas targets. The exponential decay of the  $J$ -levels of the  $1s2s2p\ ^4P_J$  state is presented in Fig. 1. The corresponding lifetimes were adopted from Ref. [13]. Similar reports exist in the literature in Refs. [14, 15, 16] and are presented in Table 1. The  $1s2s2p\ ^4P_J$  states predominantly Auger decay to the  $1s^2$  ground state since the dipole radiative decay is forbidden. It is evident that due to the inherently different lifetimes of the  $J$ -levels, especially for the  $J = 5/2$  case, the decay time axis can be separated into three

regions: Region I, where the contributions to the electron yield from the  $J = 1/2$  and  $J = 3/2$  levels is marginal and can be omitted. Thus, only contributions from the  $J = 5/2$  level may be considered. Region II, where similarly to region I contributions from the  $J = 1/2$  level may be omitted. Consequently, we may consider contributions only from  $J = 3/2$  and  $J = 5/2$  levels. Region III, where all  $J$ -levels contribute. The electron yield can be obtained as a function of the decay time that is experimentally feasible as shown later on in the manuscript. In addition to the proposed separation, the population of the  $1s2s2p\ ^4P_J$  state should be accomplished via direct processes that are not followed by secondary effects altering thus the  $J$ -levels lifetime measurement. Such collision systems are proposed later on in the manuscript as well. Then, the exponential decay law is applied to the three regions as follows:

$$Z_1 \equiv Z(J = 5/2) = A_1(5/2) e^{-t/\tau_{5/2}} \quad (1)$$

$$Z_2 \equiv Z(J = 3/2) + Z(J = 5/2) = A_2(3/2) e^{-t/\tau_{3/2}} + A_2(5/2) e^{-t/\tau_{5/2}} \quad (2)$$

$$Z_3 \equiv Z(J = 1/2) + Z(J = 3/2) + Z(J = 5/2) = A_3(1/2) e^{-t/\tau_{1/2}} + A_3(3/2) e^{-t/\tau_{3/2}} + A_3(5/2) e^{-t/\tau_{5/2}} \quad (3)$$

where  $Z(J)$  are the electron yields,  $A_i(J)$   $i = 1, 2, 3$ , the maximum populations in each region and  $\tau_J$  the lifetimes of the  $J$ -levels, respectively. Then, by fitting the data in region I with Eq. (1),  $\tau_{5/2}$  is obtained. Next, inserting this value in Eq. (2) and fitting the data of region II,  $\tau_{3/2}$  is obtained. Finally, inserting the values of  $\tau_{3/2}$  and  $\tau_{5/2}$  in Eq. (3) and fitting the data of region III,  $\tau_{1/2}$  is obtained. It was found that this splitting in three regions results in more accurate  $\tau_J$  values as opposed to a global fit of the form of Eq. (3) to the whole set of data. This is mainly due to the much longer lifetime of the  $J = 5/2$  level compared to the  $J = 1/2$  and  $J = 3/2$  levels. We should point out that the borders of the areas I, II and III are not strictly defined, but rather are part of the analysis. Indeed, in the case of experimental data, where only one decay curve is measured corresponding to the sum of all  $J$ -levels contributions, the separation of the regions could be decided upon the accuracy of the fits of Eq. (1), Eq. (2) and Eq. (3).

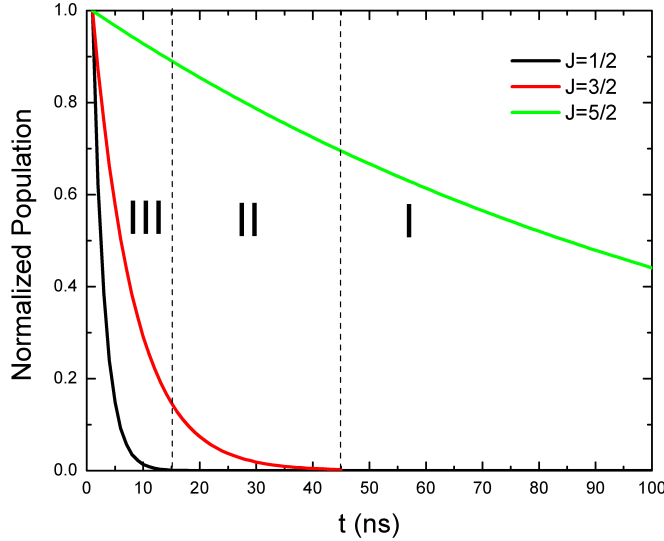


**FIGURE 1.** Exponential decay of the normalized populations of the  $J$ -levels of the  $C^{3+}(1s2s2p\ ^4P_J)$  state. The three separated regions of the method are depicted by the dashed lines.

## IMPLEMENTATION OF THE METHOD IN SIMION

The implementation of the method depends on the experimental setup (gas target geometry, spectrometer, distance between spectrometer and target, apertures, etc). In this work, the method is applied to the zero-degree Auger projectile spectroscopy (ZAPS) apparatus shown in Fig. 2. The projectile ion beam passes through a gas cell where it collides with the atoms resulting in excited ionic states. For ions with low atomic numbers these excited ionic states predominantly de-excite via Auger decay. The resulting Auger electrons, emitted at zero degrees with respect to the beam direction (the preferable angle for high resolution measurements) are energetically analyzed using the ZAPS

**TABLE 1.** Lifetimes (in ns) of the  $J$ -levels of  $1s2s2p\ ^4P_J$  state for  $3 \leq Z \leq 10$ .

Z	J	Ref. [14]	Refs. [15, 16]	Ref. [13]	Z	J	Ref. [14]	Refs. [15, 16]	Ref. [13]
3	1/2	-	-	112.04	7	1/2	1.89	1.56	1.54
	3/2	-	-	207.66		3/2	7.66	5.43	4.10
	5/2	-	-	6396.9		5/2	54.15	-	56.46
4	1/2	-	-	20.08	8	1/2	1.09	0.91	0.90
	3/2	-	-	39.82		3/2	4.40	3.34	2.50
	5/2	-	-	1062.98		5/2	28.30	27.67	29.57
5	1/2	-	6.93	6.62	9	1/2	0.67	0.57	0.56
	3/2	-	18.09	14.49		3/2	2.15	1.85	1.46
	5/2	-	297	308.89		5/2	16.16	15.90	16.83
6	1/2	3.70	3.01	2.94	10	1/2	0.42	0.37	0.36
	3/2	13.19	9.10	7.10		3/2	0.90	0.86	0.73
	5/2	117.20	-	121.36		5/2	9.79	9.77	10.29

spectrometer. This consists of a paracentric hemispherical deflector analyzer (HDA) equipped with a 4-element focusing/deceleration entry lens and a 2-dimensional position sensitive detector (PSD). For a recent description and operation of the setup see Refs. [17, 18].

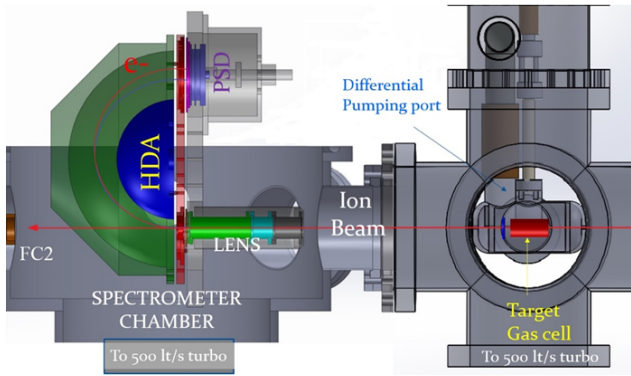


**FIGURE 2.** The ZAPS experimental setup.

Here, we used the SIMION ion optics package to simulate our proposed method for the ZAPS apparatus [19]. The ZAPS spectrometer was designed with an adequate detail of 0.5 mm per grid unit, while a code was developed in the Lua programming language for controlling all the necessary operation parameters and variables to facilitate the study. The gas cell area was replaced with a jet in order to have accurate emission position, necessary for the study but also experimentally feasible. A typical number of generated electrons per emission point was  $10^5$ . The population of the corresponding  $J$ -level at a point  $z_i$  is determined according to [11]:

$$N_J(t_i) = N_0^J e^{-t_i/\tau_J} \frac{\Delta z}{V_p \tau_J} \frac{\Delta \Omega_{J,i}}{\Delta \Omega_0} \quad (4)$$

where  $N_0^J$  is the initial population,  $\Delta z$  is the minimum step (1 mm for this study) and  $V_p$  is the velocity of the ion.  $\Delta \Omega_{J,i}$  is the solid angle defined by the emission point  $z_i$  and the entry aperture of the lens, while  $\Delta \Omega_0$  is the solid angle defined by the distance between the jet and the entry aperture of the lens.  $\Delta \Omega_{J,i}$  corresponds to long-lived states while  $\Delta \Omega_0$  to prompt states, i.e. short lifetime Auger states that decay within the gas target area.  $\Delta \Omega_0$  and  $\Delta \Omega_{J,i}$  were calculated geometrically. For the  $\Delta \Omega_{J,i}$  a maximum angle of  $2^\circ$  was applied as larger emission angles have been shown to be filtered out by the focusing lens [11]. The calculations were performed by scanning the distance between the jet and the entry lens and recording the corresponding electron signals. In order to obtain the electron yields in the form

of Eqs. 1-3, the recorded data were normalized as:

$$Z(J) \equiv N_J(t_i) \frac{\Delta\Omega_0}{\Delta\Omega_{J,i}} = N_0^J e^{-t/\tau_J} \frac{\Delta z}{V_p \tau_J} = A_J e^{-t/\tau_J}. \quad (5)$$

Note that the terms  $N_0^J$  and  $\frac{\Delta z}{V_p \tau_J}$  are constants that can be included in the state population constant  $A_J$  for fitting purposes.

The above approach was initially applied to the geometry of the aforementioned ZAPS setup in collisions of 1 MeV/amu for  $C^{3+}$  ions. However, it was realized that the current distance between the gas cell and the lens entry (289 mm) was not adequate to safely separate the  $J = 3/2$  and  $J = 5/2$  levels. Thus, during the analysis it was decided that a realistic distance for most of the cases would be the 1 m and the collision energy 0.5 MeV/amu. In this way  $J = 1/2$  and  $J = 3/2$  levels separate thoroughly while there is an adequate decay distance for the  $J = 5/2$  level. Typical fitting results for this case are shown in Fig. 3. The resulted lifetimes reproduced the initially used values with an accuracy better than 3%, that is considered adequate for the proof-of-principle of the proposed method.

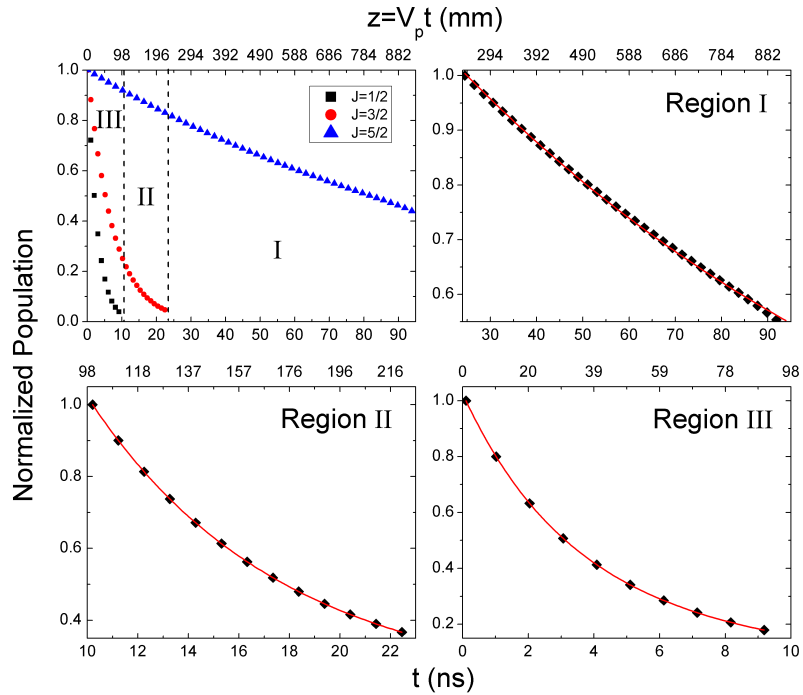


**FIGURE 3.** Normalized exponentially decaying  $J$ -levels populations for the the  $C^{3+}(1s2s2p\ 4P_J)$  state. [Top-left] The three separated regions are depicted by dashed lines. [Top-right] Region I: Contributions only from the  $J = 5/2$  level. [Bottom-left] Region II: Contributions only from the  $J = 3/2$  and  $J = 5/2$  levels. [Bottom-right] Region III: Contributions from the  $J = 1/2$ ,  $J = 3/2$  and  $J = 5/2$  levels. Red lines in Regions I, II and III correspond to the exponential decay fits according to the Eqs. 1, 2 and 3, respectively.

## EXPERIMENTAL IMPLEMENTATION

The experimental implementation of the method can be realized in the existing ZAPS apparatus imposing minor modifications. First, the gas cell should be replaced by a jet in order to have an accurate determination of the decay distances. This will not necessarily lower the measured electron yields, as compared to those from the gas cell, since larger beam sizes can be utilized to compensate for the losses. Second, a so called "J-filter", shown in Fig. 4 should be developed for the setup. This J-filter is a small size electrostatic deflector, properly grounded, that deflects all the emitted electrons prior to their entry to the J-filter. Thus, only electrons from long-lived states emitted after the J-filter will be recorded. The J-filter will scan the ion beam path from the jet to the lens entry in controlled small

steps. The electron yield can be obtained as a function of the emission point  $z_i$  after subtracting two spectra recorded at consecutive distances  $z_i$  and  $z_{i+1}$ .

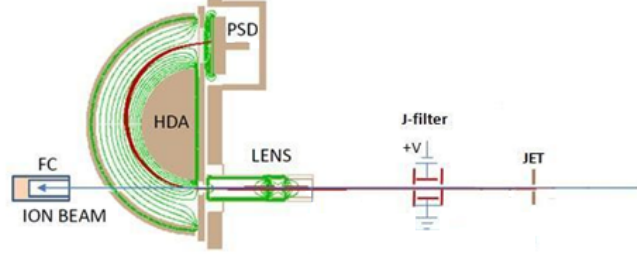


**FIGURE 4.** Proposed modification of the ZAPS setup for determining the lifetimes of the  $J$ -levels of the long-lived  $1s2s2p\ ^4P_J$  state.

The  $1s2s2p\ ^4P_J$  state can be populated in fast ion-atom collisions with various processes. However, a preferred process is the use of Be-like ions of few MeV/amu collisions with  $H_2$  targets. The reasons are two: a) These ions are routinely delivered by tandem accelerators in a mixed-state ( $1s^22s^2\ ^1S$ ,  $1s^22s2p\ ^3P$ ) content. The  $1s^22s2p\ ^3P$  state is metastable and delivered in a percentage larger than 60%, thus facilitating the efficiency of the measurement. b) The  $1s2s2p\ ^4P_J$  state is formed after single ionization of the  $1s$  electron of the  $1s^22s2p\ ^3P$  state. Thus, the state is free of any secondary processes, present in other cases (e.g. cascade effects in He-like beams), that may affect the populations in the exponential decay law. Indeed, such measurements involving mixed-state ( $1s^22s^2\ ^1S$ ,  $1s^22s2p\ ^3P$ ) beams for  $C^{2+}$  and  $O^{4+}$  were recently reported by our group [12].

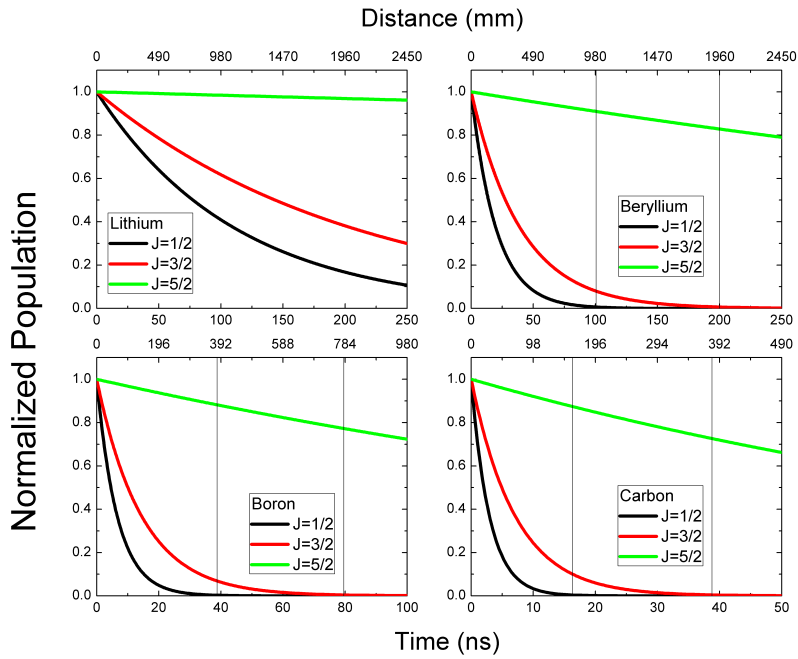


**FIGURE 5.** Normalized exponentially decaying  $J$ -levels populations for lithium, beryllium, boron and carbon. The collision energy is 0.5 MeV/amu and the distance between the jet and the lens entry is 1 m. The top x-axes indicate the decay distance measured from the jet location. The separation of the decay into three regions is depicted by grey lines.

## LIMITS OF THE APPLICABILITY OF THE METHOD

In an effort to investigate the limitations of the method we studied the  $1s2s2p\ ^4P_J$  state  $J$ -levels lifetimes for elements with atomic number  $3 \leq Z \leq 10$  using the reported in the literature lifetimes of Ref. [13]. The normalized exponentially decaying  $J$ -levels populations are shown in Figs. 5-6. A typical collision energy of 0.5 MeV/amu was used while the distance between the jet and the lens entry was set to 1 m throughout. The results are presented as a function of the decay time as well as the distance from the jet. The latter is a straightforward way to inspect the applicability of the method. Indeed, for the cases of lithium and beryllium, the very long decay times of the  $J$ -levels result in distances of a few meters that are experimentally prohibited, primarily due to the very small detection efficiency. For boron, the lifetimes are smaller and the involved distances and corresponding efficiencies are not prohibitive. Therefore we consider it as a lower  $Z$  limit for the implementation of the method. Based on the decay distances shown in Figs. 5-6 the method seems to be easily applicable for the rest elements, i.e. for carbon, nitrogen, oxygen and fluorine, while it becomes more tedious for neon. In the latter case an even lower collision energy would favour the method.

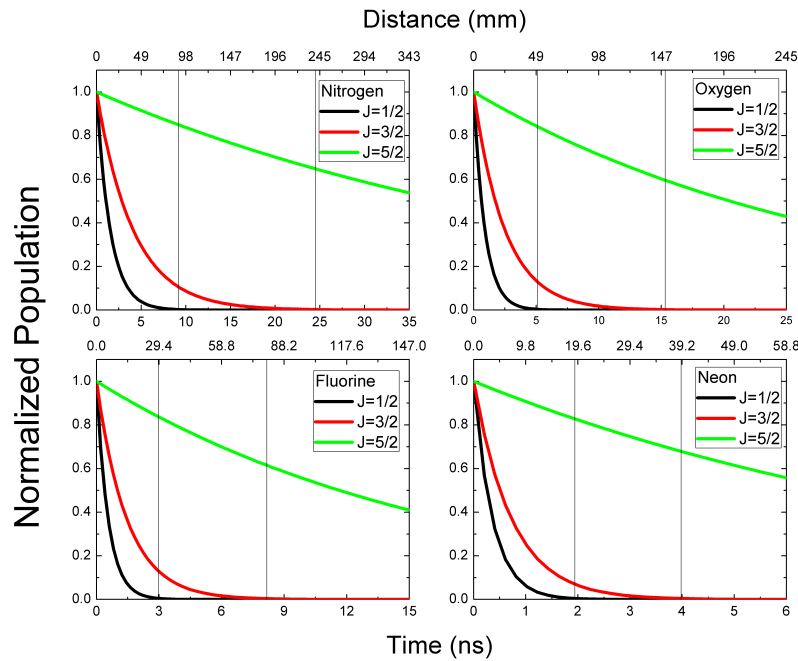


**FIGURE 6.** Same as in Fig. 5 but for nitrogen, oxygen, fluorine and neon.

## CONCLUSIONS

A method has been proposed for the measurement of  $J$ -levels lifetimes of the  $1s2s2p\ ^4P_J$  long-lived state for Li-like ions. The method was implemented utilizing Monte Carlo type simulations within the SIMION ion optics simulation package for the ZAPS apparatus located at NCSR "Demokritos" Tandem accelerator laboratory. The study was applied to  $C^{3+}$  ions where the resulted lifetimes reproduced the initially used values with an accuracy better than 3%, that is considered adequate for the proof-of-principle of the proposed method. The study was extended as to include the lifetimes of elements with atomic numbers  $3 \leq Z \leq 10$ . A typical collision energy 0.5 MeV/amu and a distance between the jet gas target and the entry aperture of the lens of 1 m seemed most adequate for the applicability of the method, except for the lithium and beryllium cases. An experimental realization of the method has been also proposed making use of a "J-filter" mechanism that selects the electron yield as a function of the decay distance. Finally, the use of few MeV/amu Be-like ions in the mixed-state ( $1s^22s^2\ ^1S$ ,  $1s^22s2p\ ^3P$ ) in collisions with  $H_2$  targets is suggested as the candidate for the corresponding studies.

## ACKNOWLEDGMENTS

We acknowledge support of this work by the project "Cluster of Accelerator Laboratories for Ion-Beam Research and Applications - CALIBRA" (MIS 5002799) which is implemented under the Action "Reinforcement of the Research and Innovation Infrastructure", funded by the Operational Programme "Competitiveness, Entrepreneurship and Innovation" (NSRF 2014-2020) and co-financed by Greece and the European Union (European Regional Development Fund).

## REFERENCES

- [1] T. J. M. Zouros and D. H. Lee, in Accelerator-Based Atomic Physics Techniques and Applications, edited by S. M. Shafroth and J. C. Austin (American Institute of Physics Conference Series, Woodbury, NY, 1997) Chap. 13., pp. 426–479.
- [2] T. J. M. Zouros, B. Sulik, L. Gulyas, and K. Tokesi, *Phys. Rev. A* **77**, p. 050701 (2008).
- [3] D. Strohschein, D. Röhrbein, T. Kirchner, S. Fritzsche, J. Baran, and J. A. Tanis, *Phys. Rev. A* **77**, p. 022706 (2008).
- [4] D. Röhrbein, T. Kirchner, and S. Fritzsche, *Phys. Rev. A* **81**, p. 042701 (2010).
- [5] E. P. Benis, S. Doukas, and T. J. M. Zouros, *Nucl. Instrum. Methods Phys. Res. B* **369**, 83 – 86 (2016).
- [6] E. P. Benis and T. J. M. Zouros, *J. Phys. B* **49**, p. 235202 (2016).
- [7] M. Zamkov, H. Aliabadi, E. P. Benis, P. Richard, H. Tawara, and T. J. M. Zouros, *Phys. Rev. A* **64**, p. 052702 (2001).
- [8] M. Zamkov, E. P. Benis, P. Richard, and T. J. M. Zouros, *Phys. Rev. A* **65**, p. 062706 (2002).
- [9] E. P. Benis, M. Zamkov, P. Richard, and T. J. M. Zouros, *Phys. Rev. A* **65**, p. 064701 (2002).
- [10] D. H. Lee, P. Richard, J. M. Sanders, T. J. M. Zouros, J. L. Shinpaugh, and S. L. Varghese, *Nucl. Instrum. Methods Phys. Res. B* **56/57**, p. 99 (1991).
- [11] S. Doukas, I. Madesis, A. Dimitriou, A. Laoutaris, T. J. M. Zouros, and E. P. Benis, *Rev. Sci. Instrum.* **86**, p. 043111 (2015).
- [12] E. Benis, I. Madesis, A. Laoutaris, S. Nanos, and T. Zouros, *J. Electron Spectrosc. and Relat. Phenom.* **222**, 31 – 39 (2018).
- [13] E. P. Benis, S. Doukas, T. J. M. Zouros, P. Indelicato, F. Parente, C. Martins, J. P. Santos, and J. P. Marques, *Nucl. Instrum. Methods Phys. Res. B* **365**, 457 – 461 (2015).
- [14] M. H. Chen, B. Crasemann, and H. Mark, *Phys. Rev. A* **27**, 544–547 (1983).
- [15] B. F. Davis and K. T. Chung, *Phys. Rev. A* **36**, p. 1948 (1987).
- [16] B. F. Davis and K. T. Chung, *Phys. Rev. A* **39**, 3942–3955 (1989).
- [17] I. Madesis, A. Dimitriou, A. Laoutaris, A. Lagoyannis, M. Axiotis, T. Mertzimekis, M. Andrianis, S. Harisopulos, E. P. Benis, B. Sulik, I. Valastyán, and T. J. M. Zouros, *J. Phys: Conf. Ser.* **583**, p. 012014 (2015).
- [18] A. Dimitriou, A. Laoutaris, I. Madesis, S. Doukas, E. P. Benis, B. Sulik, O. Sise, A. Lagoyannis, M. Axiotis, and T. J. M. Zouros, *J. Atom. Mol. Cond. Nano Phys.* **3**, 125–131 (2016).
- [19] <http://www.simion.com> .